



A paper-based optical probe for chromium by using gold nanoparticles modified with 2,2'-thiodiacetic acid and smartphone camera readout

Shadab Faham¹ · Gholamreza Khayatian¹ · Hamed Golmohammadi² · Raouf Ghavami¹

Received: 11 March 2018 / Accepted: 17 June 2018 / Published online: 13 July 2018
© Springer-Verlag GmbH Austria, part of Springer Nature 2018

Abstract

A paper based analytical device is presented for the determination of Cr(III) and Cr(VI) using gold nanoparticles (AuNPs) modified with 2,2'-thiodiacetic acid. The modified AuNPs were characterized using UV-Vis spectrophotometry, Fourier transform infrared, dynamic light scattering, zeta potential, energy dispersive spectroscopy and transmission electron microscopy. Cr(III) ions induce the aggregation of the modified AuNPs, and the color of the nanoprobe changes from red to blue. This can be detected visually, or by colorimetry, or with a camera. No interference is observed in the presence of 19 other cations and anions. Cr(VI) (chromate) can be determined by after reduction to Cr(III) by using ascorbic acid and then quantified total Cr(III). The concentration of Cr(VI) is obtained by subtracting the concentration of Cr(III) from that of total chromium. Under optimal conditions, the ratio of the absorbances measured at 670 (blue) and 522 (red) increases linearly in the 1.0 nM to 22.1 μM chromium concentration range, with 0.66 nM (0.034 ppb) limit of detection (LOD) in solution. In case of the paper device, the linear range extends from 1.0 nM to 0.1 mM, and the LOD is 0.64 nM (0.033 ppb). The method was applied to the determination of chromium in spiked water, urine and dilutes human plasma, and results were confirmed by GF-AAS analysis. This method is highly selective, fast and portable, requires minimum volume of reagents and samples and no washing steps.

Keywords AuNPs · 2,2'-Thiodiacetic acid · Paper based analytical device · Cr(III) · Cr(VI)

Introduction

Chromium(III) ion in low concentration acts as a cofactor for the action of insulin to regulate sugar levels, but high concentrations of Cr(III) can cause DNA damage, genetic lesions and cell mutation. Hexavalent chromium (chromate) is even more toxic. It causes health problems such as injury in the nasal septum, skin allergies, gastrointestinal effects, kidney and liver damage and cancer in various organs. The World Health Organization has set maximum permissible level of Cr(VI) in drinking water as 0.05 mg L⁻¹ [1, 2].

Electronic supplementary material The online version of this article (<https://doi.org/10.1007/s00604-018-2875-6>) contains supplementary material, which is available to authorized users.

✉ Gholamreza Khayatian
gkhatatian@uok.ac.ir; gkhatatian@yahoo.com

¹ Department of Chemistry, Faculty of Science, University of Kurdistan, P.O. Box 416, Sanandaj 66177-15175, Iran

² Chemistry and Chemical Engineering Research Center of Iran, Tehran 14335-186, Iran

Electrothermal atomic absorption spectrometry (ETAAS) [3], HPLC-ICP-MS [4], fluorescent [5] and electrochemical analysis [6] are common methods for the determination of chromium in various real samples. However, these methods often require sample preparation and complicated equipment. Colorimetric methods by using AuNPs and AgNPs have become attractive because they can easily be detected visually or by UV-Vis spectrophotometry [7].

Gold nanoparticles have been reported as probes for heavy metal ions [8], DNA [9] and protein [10] assays. Surface plasmon band shifts to longer wavelength and the color solution is change from red to blue due to the aggregation of AuNPs in the presence of target. For example, a colorimetric probe using tyrosin-AuNPs has been developed for simultaneous determination of Cr(III) and Pb(II) [11]. Also mercaptosuccinic acid [12] and 4-amino-5-methyl-4H-1,2,4-triazole-3-thiol [13] can be used to promote the aggregation of AuNPs in the presence of Cr(III). Nanodiamonds@AuNPs can be considered as a colorimetric probe for the determination of clenbuterol and Cr(III) ions in water and urine samples [14]. A colorimetric paper-based on non-aggregation of AuNPs was presented for Cr(VI) assay in water samples [15].

A paper-based or lab-on-paper analytical method was first applied for bioassay by Whitesides's group in 2007 [16]. Paper was applied in colorimetric, fluorescent and electrochemical methods due to its outstanding features including low price, proper porosity, biocompatibility, biodegradability and flexibility [17, 18]. Portable, fast and low-cost paper-based methods are preferred to time-consuming laboratory analysis. They are widely used for point of care medical diagnostics [19] and environmental analysis [20].

The Chromium measurements in urine and plasma can be a reliable marker for chromium exposure [21, 22]. For this purpose, a straightforward and low-cost analysis for Cr(III) assay is lab-on-paper colorimetric method.

We have developed an efficient TDA-AuNPs probe for the determination of Cr(III) and Cr(VI) in a paper based analytical device. The aim of this study is to design a portable and miniaturized method for monitoring Cr in biofluids and on-site environmental analysis. The TDA-AuNPs were characterized using various identification techniques. The color of TDA-AuNPs probe changed from red to blue upon addition of Cr(III) which can be monitored by the bare eye, UV-Vis spectrophotometry or with a smartphone camera. Under optimal conditions, this method exhibited high selectivity, low detection limit and a wide linear range for speciation of Cr(III) and Cr(VI).

Experimental

Reagents and chemicals

Chloroauric acid trihydrate ($\text{HAuCl}_4 \cdot 3\text{H}_2\text{O}$), tri-sodium citrate dehydrate, $\text{Cu}(\text{NO}_3)_2$, $\text{Cd}(\text{NO}_3)_2$, $\text{Pb}(\text{NO}_3)_2$, $\text{Co}(\text{NO}_3)_2$, $\text{Ni}(\text{NO}_3)_2$, AgNO_3 , $\text{Al}(\text{NO}_3)_3$, $\text{Fe}(\text{NO}_3)_3$, $\text{Mg}(\text{NO}_3)_2$, $\text{Ca}(\text{NO}_3)_2$ and $\text{Cr}(\text{NO}_3)_3$ were purchased from Merck (Darmstadt, Germany, www.merck.com) and 2,2'-thiodiacetic acid (TDA), NaNO_3 , $\text{Zn}(\text{SO}_4)_2$, $\text{Fe}(\text{SO}_4)_2$, $\text{Mn}(\text{SO}_4)_2$, Na_2SO_4 , $\text{K}_2\text{Cr}_2\text{O}_7$, HgCl_2 , KBr , KCl , Triton X-100, nitric acid (65%), ascorbic acid, acetic acid, boric acid and sodium hydroxide were purchased from Sigma-Aldrich company (www.sigmaaldrich.com). Doubly distilled-deionized water was used in all the experiments.

Instrumentation

The UV-Vis spectrometry measurements were performed using an Analytic Jena Specord 210 spectrophotometer (www.analytik-jena.com, Germany). Elemental analysis was obtained with an EDS Sirius SD. Transmission electron microscopy (TEM) images were recorded with a Zeiss-EM10 Cooperated at 80 keV. Fourier transform infrared spectra were recorded on a Vector 22 BRUKER spectrophotometer (Germany). A Varian

spectra 220 (Australia) atomic absorption spectrometer equipped with a deuterium background correction system and electrothermal atomizer, GTA-110 was used for chromium determination. Dynamic light scattering (DLS) was measured via a Malvern Zetasizer-nano zs (England). The pH measurements were carried out using Metrohm 713 model pH-meter (with precision of ± 1 mV) furnished with a combined glass-saturated calomel electrode. The photos were taken with a Samsung Galaxy E5 mobile phone.

Preparation of AuNPs and TDA-AuNPs

AuNPs were prepared by reducing HAuCl_4 with tri-sodium citrate in the aqueous phase [23]. Briefly, tri-sodium citrate (25 mL, 38.8 mM) was added to a boiling solution of HAuCl_4 (250 mL, 1.0 mM). After 30 min, a wine-red solution was obtained.

For the preparation of TDA-AuNPs, the AuNPs (250 mL) were incubated with a 12.5 mL of 0.01 mM TDA aqueous solution under stirring in a dark place for 2 h. The TDA molecules were capped on AuNPs through ligand exchange with citrate via -S- atoms. A very stable dispersed solution was obtained. The solutions were centrifuged to remove free agents. The TDA-AuNPs were stored at 4 °C and remained stable for more than 6 months.

Speciation of chromium

First, Cr(VI) ions were reduced to Cr(III) with 2.0 mM ascorbic acid for 30 min [24]. Then, the colorimetric assay procedure for Cr(III) was repeated for total Cr determination. The concentration of Cr(VI) was obtained by subtracting the concentration of Cr(III) from the total chromium.

Urine and human serum plasma samples

For colorimetric assay, 100 μL of the urine and human serum plasma were treated with 20 μL of nitric acid 0.2 M. The treated solutions were diluted 50 times.

For graphite furnace atomic absorption spectrometry (GF-AAS), 100 μL of the biofluids were treated with 20 μL of nitric acid 0.2 M. Then each treated urine and human serum plasma samples were mixed separately with 20 μL of HNO_3 (1%) and Triton X-100 (1%) as modifier, respectively. The resulting samples were introduced to GF-AAS [25].

Results and discussion

Choice of material

AgNPs and AuNPs exhibit a size dependent optical property known as surface plasmonic effect, which has a strong UV-

visible absorption band located in the visible region. The use of AuNPs has been more popular than AgNPs because AuNPs are easier modified with one or more sulfur moieties and are chemically more stable than AgNPs. The TDA molecule was a favorable choice for chromium determination because of its water solubility and due to hard nature of two basic COO^- groups can offer strong interaction with hard acid such as Cr^{3+} .

Characterization of TDA-AuNPs

As shown in Fig. S1A, the TDA-AuNPs exhibited SPR absorption at 522 nm. Fig. 1a and b show the FT-IR spectra of citrate and AuNPs-citrate, respectively. The presence of C=O, C-O and OH in Fig. 1b demonstrates that citrate may be capped on the surface of AuNPs. The C-O peak of citrate at 1276 cm^{-1} in Fig. 1a shifts to 1242 cm^{-1} in Fig. 1b. This probably indicates that C-O interacts with AuNPs and the band weakens and hence shifts to lower frequency. In addition, Fig. 1c and d illustrate the FT-IR spectra of pure TDA and TDA-AuNPs, respectively. In Fig. 1c, the very broad peak at $3100\text{--}2030\text{ cm}^{-1}$ may be due to OH stretching of carboxylic acids. The peak at 2910 cm^{-1} can be attributed to the stretching of aliphatic $-\text{CH}_2$ groups. The peak at 1693 cm^{-1} is due to C=O stretching of carboxylic acids. The shift of C=O from 1693 cm^{-1} (Fig. 1c) to 1593 cm^{-1} in Fig. 1d shows that the TDA agent may be capped on the surface of AuNPs. According to these results, the capping of citrate and TDA on the surface of AuNPs can be separately identified. However, a comparison of Fig. 1b and d shows that AuNPs-citrate and TDA-AuNPs have similar spectra. This method has not been able to differentiate between them. Therefore, the ligand exchange of citrate to TDA is not confirmed by FT-IR. This can be due to the low concentration of TDA used in our study. A comparison of Fig. 1d and e indicates the FT-IR spectrum of TDA-AuNPs and TDA-AuNPs in the presence of $50\text{ }\mu\text{M Cr(III)}$, respectively. As can be seen, the C=O band at 1593 cm^{-1} (Fig. 1d) shifts to lower frequency (1587 cm^{-1}) in Fig. 1e which can be due to interaction of Cr(III) with TDA-AuNPs. According to hard-soft acid-base (HSAB) theory, the hard acid Cr(III) tend to interact with hard base (oxygen atoms

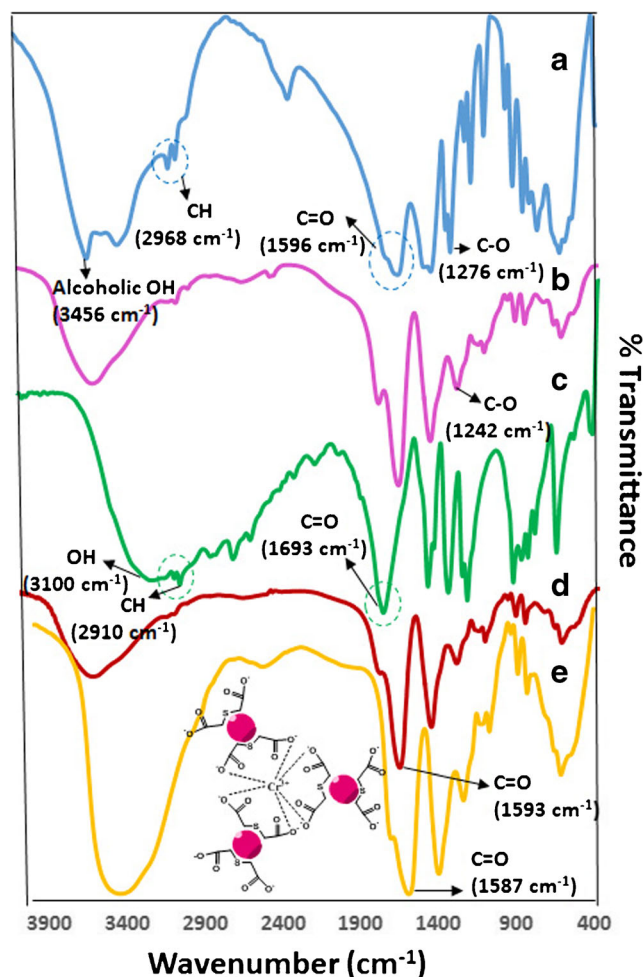


Fig. 1 FT-IR spectra of (a) citrate, (b) AuNPs-citrate, (c) TDA, (d) TDA-AuNPs and (e) TDA-AuNPs in the presence of $50\text{ }\mu\text{M Cr(III)}$

in COO^- groups). After interaction of Cr(III) with AuNPs, the double band character of C=O decreases and thus a shift to lower frequency is observed.

We studied the ligand exchange of citrate with TDA using EDS, TEM and zeta potential analysis. The EDS spectrum of TDA-AuNPs shows carbon, oxygen, sulfur and gold peaks (Fig. S1B). The presence of sulfur in the EDS spectrum confirmed the presence of TDA on the surface of AuNPs. Characterization of AuNPs-citrate and AuNPs-TDA core-shell nanoparticles were

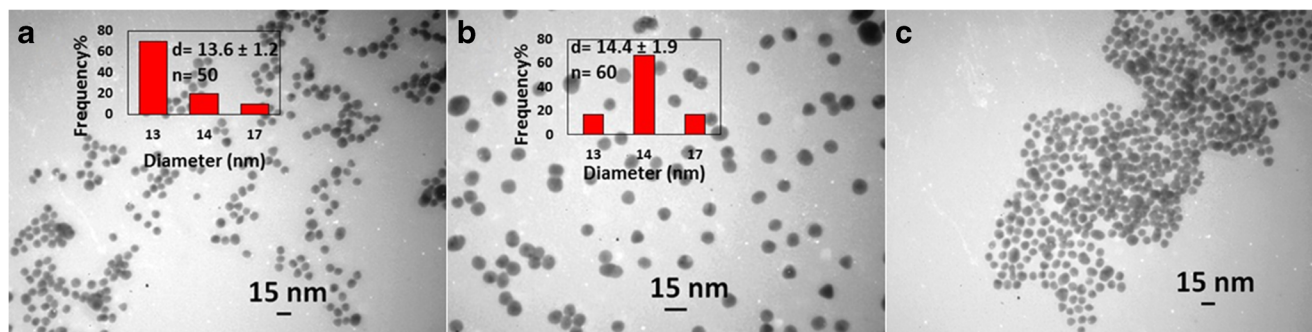
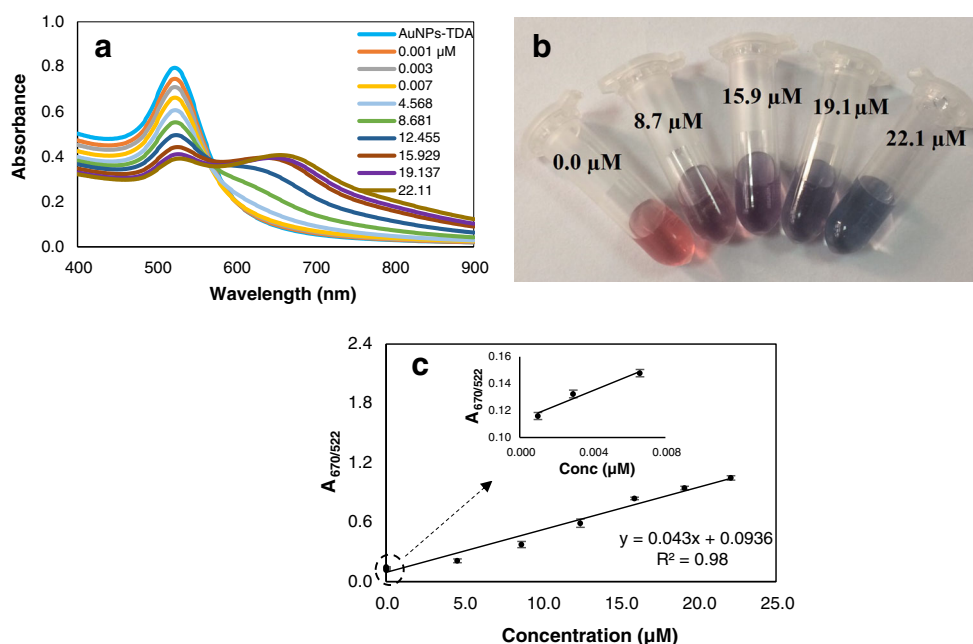


Fig. 2 (a) TEM image of AuNPs-citrate, (b) TEM images of TDA-AuNPs in the absence and (c) in the presence of $10\text{ }\mu\text{M Cr(III)}$

Fig. 3 (a) UV-Vis absorption spectra and (b) Visual color changes of TDA-AuNPs upon addition of Cr(III) in the concentration range of 1.0 nM–22 μ M, (c) Plot of the $A_{670/522}$ values of TDA-AuNPs versus Cr(III) concentration



investigated using TEM. The citrate shell around AuNPs was not clear in the TEM image (Fig. 2a). However, the TDA shell around AuNPs was determined at 2.3 nm (Fig. S2). As a result, the presence of TDA shell around AuNPs confirmed the ligand exchange of citrate to TDA. The zeta potentials of AuNPs-citrate and TDA-AuNPs were -13.9 and -31.8 (Fig. S3D and E). The TDA-AuNPs had -17.9 times more negative charge than AuNPs-citrate and were more stable. As shown in the TEM image, the TDA-AuNPs are spherical and well dispersed in aqueous solution with an average size of 14.4 ± 1.9 nm for $n = 60$ (Fig. 2b). The TEM image of TDA-AuNPs in the presence of $10.0 \mu\text{M}$ Cr(III) shows that TDA-AuNPs aggregated to large

particles (Fig. 2c). Furthermore, the average hydrodynamic diameter of TDA-AuNPs was obtained at 19.97 (Fig. S3B) with a dispersity index of 0.556 by DLS analysis. The average hydrodynamic diameter of TDA-AuNPs increased to 41.05 in the presence of Cr(III) (Fig. S3C). Increasing hydrodynamic diameter showed that Cr(III) induces the aggregation of AuNPs. The zeta potentials of AuNPs-citrate, TDA-AuNPs and TDA-AuNPs in the presence of $10.0 \mu\text{M}$ Cr(III) were -13.9 , -31.8 and -28.5 , respectively (Fig. S3D-F). The TDA was deprotonated at $\text{pH} = 5.0$ acetate buffer (TDA, $\text{pK}_{a1} = 3.14$ and $\text{pK}_{a2} = 4.01$ [26]). The TDA-AuNPs were more stable than AuNPs-citrate due to more negative TDA ions capped on the AuNPs than citrate ions. The negative charge of TDA-AuNPs decreased in the presence of Cr(III) due to complexation which leads to low stability and therefore aggregation of nanoparticles.

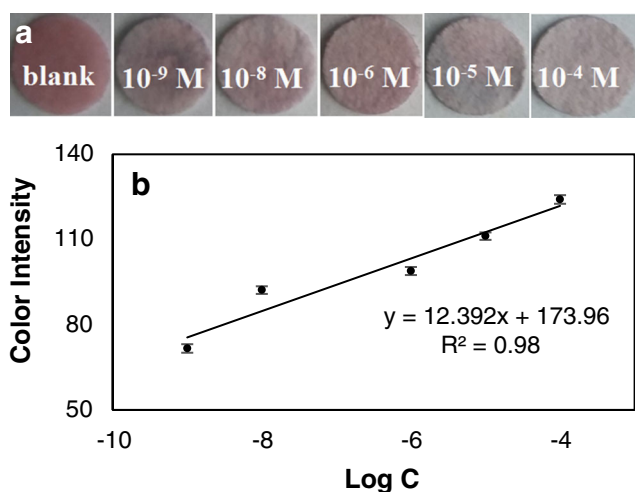
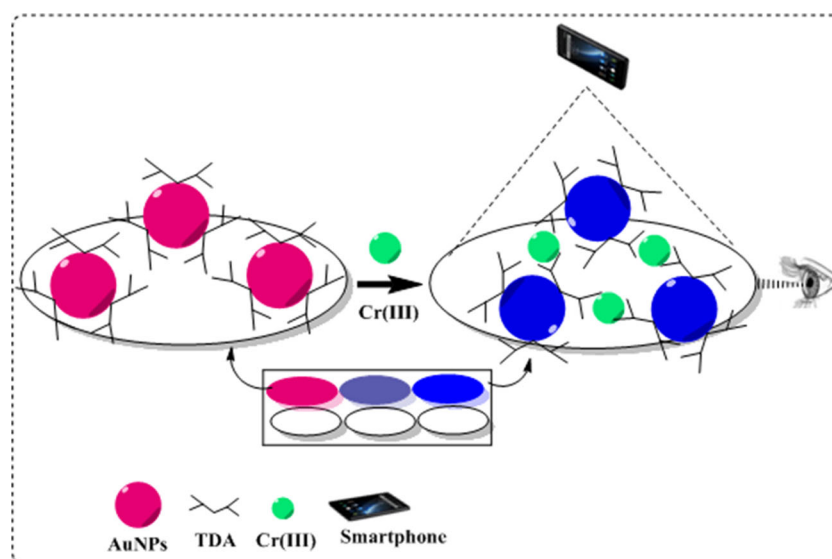


Fig. 4 (a) Photographs of TDA-AuNPs spots on the paper in the presence of different concentrations of Cr(III) in the range of 1.0 nM– 0.1 mM, (b) Linear calibration for color intensity versus logarithm concentration of Cr(III)

Dynamic light scattering (DLS) and zeta potential analysis

Fig. S3, illustrates determination of the average hydrodynamic size, polydispersity indices and zeta potentials. The polydispersity indices for AuNPs-citrate, TDA-AuNPs and TDA-AuNPs-Cr(III) were 0.519 , 0.556 and 0.552 , respectively. It is noteworthy that the polydispersity of AuNPs-citrate and TDA-AuNPs were a bit slightly higher when compared to each other, as a possible result of a few larger nanoparticles. The DLS method is based on light scattering. The intensity of the light scattered by particles enhances as the sixth power of the diameter and the signal is prevailed by the largest particles; this means that when samples contain the small and large nanoparticles, the small ones cannot be detected [27].



Scheme 1 The mechanism of paper analytical device based on TDA-AuNPs for Cr(III) assay

Therefore, the samples with high polydispersity cannot be evaluated using DLS alone. Electron microscopy is another method that is less sensitive to polydispersity. Thus, we supported our results by TEM technique. As shown in Fig. 2b, the TEM image of TDA-AuNPs in the absence of Cr(III) shows good dispersion. In addition, the zeta potential of TDA-AuNPs is high, approximately -31.8 (Fig. S3E). Therefore, the TDA-AuNPs are stable because the strong electrostatic repulsion between the nanoparticles prevents their aggregation.

Colorimetric assay for Cr(III) in solution

For Cr(III) assay, 0.5 mL of acetate buffer with pH = 5.0 was mixed with 100 μL of TDA-AuNPs. Then, different concentrations of Cr(III) were added to this solution. UV-Vis absorption spectra were recorded after 5 min at room temperature. The addition of Cr(III) to TDA-AuNPs

solutions led to the red shift in its SPR band as shown in Fig. 3a. Depending on the concentration of Cr(III), the color of solution was changed from red to purple, and in the higher concentrations to blue (Fig. 3b). The aggregation of TDA-AuNPs was induced by interaction between oxygen groups in TDA with Cr(III). The decrease interparticle distance between nanoparticles lead to a remarkable red shift in the LSPR band and a visual color change from red to blue. A linear correlation was obtained between $A_{670/522}$ and Cr(III) concentration in the range of 1.0 nM–22.1 μM with LOD = 0.66 nM. The relative standard deviations (RSDs) of the colorimetric method were in the range of 1.4–8.7% which demonstrated the good repeatability of this method. As shown in the TEM image, the TDA-AuNPs are well-dispersed in the absence of Cr(III) (Fig. 2b), but aggregated together in the presence of 10.0 μM Cr(III) (Fig. 2c). These results confirm that Cr(III) is induced the aggregation of TDA-AuNPs.

Table 1 Comparison of this method with some reported studies

Methods	Probe	Analyte	LOD	Linear range	Ref.
Colorimetric	DMSA-AuNPs	Cr(III) and $\text{Cr}_2\text{O}_7^{2-}$	10 nM	10–500 nM	[28]
Colorimetric	PAH-AuNPs	Cr(III)	1.17 μM	5.0–120 μM	[29]
Colorimetric	Tween 20-AuNP	Cr (III)	0.016 μM	0.5–5.0 μM	[30]
Colorimetric	SH-AuNPs	Cr(III)	0.009 μM	0.02–2.5 μM	[31]
		Cr(VI)	0.78 nM	0.005–1.0 μM	
ET-AAS	–	Cr(III) and Cr(VI)	0.02 ng mL^{-1}	0.05–5 ng mL^{-1}	[32]
Paper-based colorimetric	AuNPs	Cr(III)	0.106 μM	1.0–1000 μM	[33]
Colorimetric	DTPA-AuNPs	Cr(III)	0.05 μM	0.07–0.40 μM	[34]
		Cr(VI)	0.005 μM	0.01–0.25 μM	
Fluorescent	g-C3N4 NS	Cr(VI) and Cr(III)	3 nM	0.01–100 μM	[35]
Paper-based colorimetric	TDA-AuNPs	Cr(III) and Cr(VI)	0.64 nM	1.0 nM–0.1 mM	This work

Lab-on-paper based assay for Cr(III)

A 10 μL of TDA-AuNPs with $\text{pH} = 5.0$ were spotted on punched filter papers, and the spotted papers were dried at room temperature for 20 min. This work was repeated twice. The TDA-AuNPs spots on the paper were interacted with different concentrations of Cr(III). Depending on the concentration of Cr(III), the color was changed from red to blue. The photographs of TDA-AuNPs spots on the paper were taken with a Samsung E5 mobile phone (Fig. 4a). Color intensities were calculated using Adobe photoshop CS5. The mechanism of lab-on-paper colorimetric assay for Cr(III) is shown in

Scheme 1. A linear correlation was obtained between color intensities and the logarithm of Cr(III) concentration in the range of 1.0 nM-0.1 mM with a correlation coefficient (R^2) of 0.98, and $\text{LOD} = 0.64$ nM for paper based colorimetric assay (Fig. 4b). Table 1 provides a comparison of our results with some reported studies.

Optimization of method

The following parameters were optimized: A) TDA concentration; B) Sample pH value; C) Incubation time. Respective data and Figures are given in Fig. S4. The following

Fig. 5 (a) UV-Vis absorption spectra (b) Visual color changes and (c) The $A_{670/522}$ values of TDA-AuNPs in the presence of 16.7 μM Cr(III) and 10.0 fold other cations and anions, (d) Selectivity on the paper upon addition of 10 μM Cr(III) and 10.0 fold other cations and anions

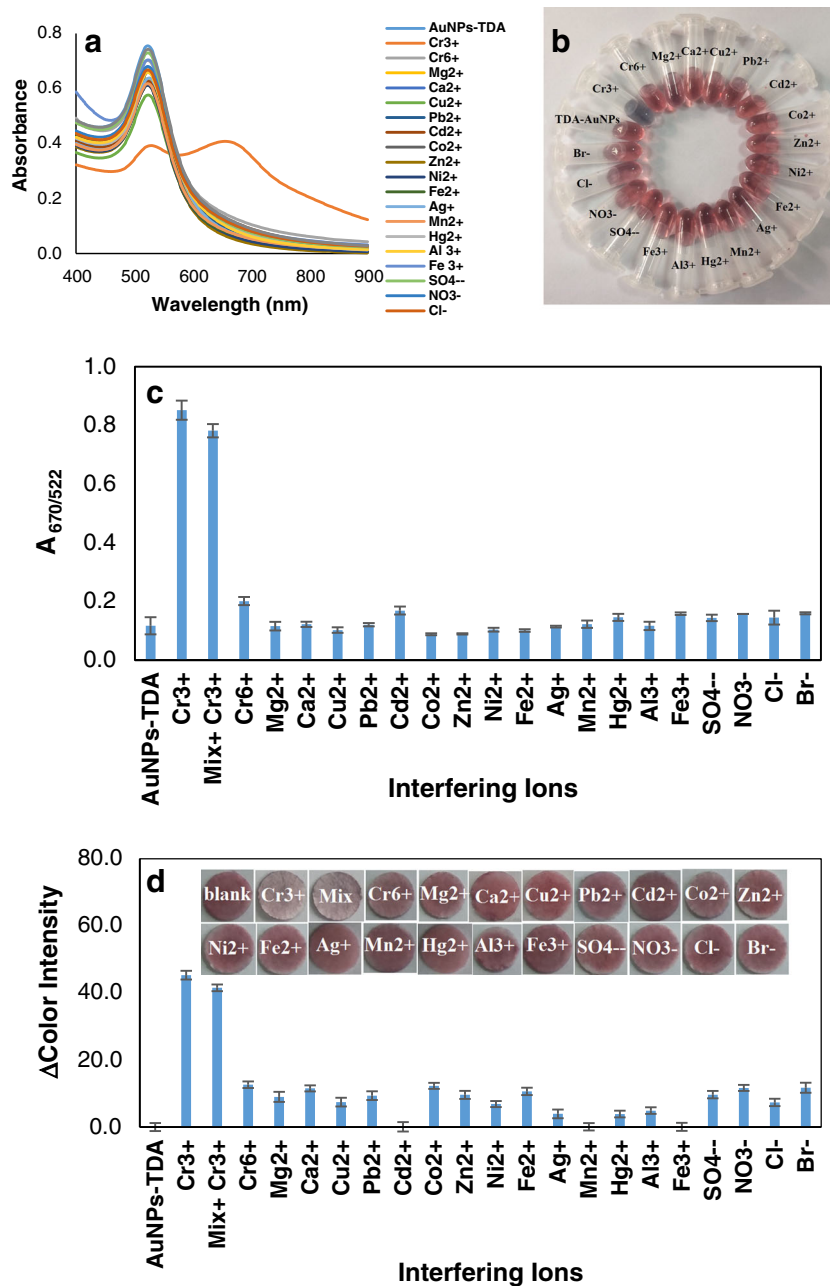


Table 2 Determination of Cr(III) and total chromium ions in real samples

Sample	Added (ppb)		Founded (ppb)		Recovery (%) (n = 3)		RSD (%) (n = 3)		GF-AAS ^a		RSD (%) (n = 3)	
	Cr(III)	Cr(VI)	Cr(III)	Cr(VI)	Cr(III)	Cr(VI)	Cr(III)	Cr(VI)	Cr(III)	Cr(VI)	Cr(III)	Cr(VI)
Tap water	0	0	0	0	–	–	–	–	1.0	–	–	–
	40	0	37.9	0	94.7	–	–5.3	–	35.0	–	8.3	–
	40	34	37.9	36.0	–	105.9	–	5.9	–	33.0	–	9.1
River water	0	0	0	0	–	–	–	–	–	–	–	–
	40	0	39.0	0	97.6	–	–2.5	–	38.0	–	–5.0	–
	40	34	39.0	34.8	–	102.4	–	2.4	–	35.5	–	3.8
Urine	0	0	0	0	–	–	–	–	1.05	–	–	–
	40	0	36.5	0	91.4	–	–8.7	–	43.2	–	6.8	–
	40	34	36.5	34.5	–	101.4	–	1.4	–	35.0	–	2.9
Human serum plasma	0	0	0	0	–	–	–	–	5.24	–	–	–
	40	0	37.0	0	92.5	–	–7.5	–	44.1	–	8.6	–
	40	34	37.0	34.6	–	101.9	–	1.9	–	36.1	–	6.2

^a Graphite furnace atomic absorption spectrometry

experimental conditions were found to give best results: A) Optimal TDA concentration: 0.5 μ M; B) Best sample pH value: 5.0 and C) Best incubation time: 5 min.

Interference study

Colorimetric assay was studied in the presence of 16.7 μ M Cr(III) and 10.0 fold of 19 other cations and anions including Cu²⁺, Cd²⁺, Pb²⁺, Co²⁺, Ni²⁺, Ag⁺, Hg²⁺, Mn²⁺, Zn²⁺, Al³⁺, Fe³⁺, Mg²⁺, Ca²⁺, Na⁺, Fe²⁺, SO₄²⁻, Cr₂O₇²⁻, Br⁻ and Cl⁻. As can be seen from Fig. 5(a-c), the remarkable red shift in the UV-Vis spectra and a visual color change generated by Cr(III) shows the selectivity of the colorimetric method. Also we demonstrate the selectivity of paper-based method for Cr(III) in Fig. 5d.

Real samples

The probe was evaluated for the measurement of Cr(III) and total chromium in water, urine and plasma samples using standard addition method and the results were compared with GF-AAS as the standard method. A good agreement can be seen between our results and GF-AAS standard method. The results are presented in Table 2. Speciation analysis of Cr(VI) and Cr(III) was performed, as described in Experimental section. As shown in Table 2, the recoveries were obtained in the range of 91.4–105.9% and RSDs in most cases are lower than 8.7%. The findings indicate that the matrix real samples did not have any interference for speciation of Cr(III) and Cr(VI) specially in water samples.

Conclusion

For biomonitoring study, we developed a TDA-AuNPs probe in paper based analytical device as a marker for chromium exposure in biofluids and also for on-site analysis in water samples. This method is fast, low-cost and portable with high sensitivity and selectivity. It can be used with a portable smartphone detector and does not require any complicated equipment. The addition of Cr(III) to the TDA-AuNPs spots on the paper lead to a change in SPR band of AuNPs and consequently the color changed from red to blue. Images of TDA-AuNPs spots on the paper were taken with a smartphone. A linear correlation was obtained between color intensity and the logarithm concentration of Cr(III) with LOD = 0.64 nM. Selectivity of the TDA-AuNPs probe was confirmed against different cations and anions. Finally, this method has provided a convenient approach for the determination of Cr(III) and total chromium in real samples.

Acknowledgments The authors are grateful for the financial support of the University of Kurdistan for this study.

Compliance with ethical standards The author(s) declare that they have no competing interests.

References

1. Biswas P, Kam AK, Balasubramanian P, Kale PG (2017) Biosensor for detection of dissolved chromium in potable water: a review. *Biosens Bioelectron* 94:589–604

2. Cárdenas-González M, Osorio-Yáñez C, Gaspar-Ramírez O, Pavković M, Ochoa-Martínez A, López-Ventura D, Medeiros M, Barbier OC, Pérez-Maldonado IN, Sabbisetti VS, Bonventre JV (2016) Environmental exposure to arsenic and chromium in children is associated with kidney injury molecule-1. *Environ Res* 150: 653–662
3. López-García I, Muñoz-Sandoval MJ, Hernández-Córdoba M (2017) Cloud point microextraction involving graphene oxide for the speciation of very low amounts of chromium in waters. *Talanta* 172:8–14
4. Araujo-Barbosa U, Peña-Vazquez E, Barciela-Alonso MC, Ferreira SLC, dos Santos AMP, Bermejo-Barrera P (2017) Simultaneous determination and speciation analysis of arsenic and chromium in iron supplements used for iron-deficiency anemia treatment by HPLC-ICP-MS. *Talanta* 170:523–529
5. Peng G, He Q, Lu Y, Huang J, Lin JM (2017) Flow injection microfluidic device with on-line fluorescent derivatization for the determination of Cr (III) and Cr (VI) in water samples after solid phase extraction. *Anal Chim Acta* 955:58–66
6. Alizadeh T, Rafiei F, Hamidi N, Ganjali MR (2017) A new electrochemical sensing platform for Cr (III) determination based on nanostructured Cr (III)-imprinted polymer-modified carbon composite electrode. *Electrochim Acta* 247:812–819
7. Mohammadi S, Khayatian G (2015) Highly selective and sensitive photometric creatinine assay using silver nanoparticles. *Microchim Acta* 182:1379–1386
8. Leng Y, Li Y, Gong A, Shen Z, Chen L, Wu A (2013) Colorimetric response of dithizone product and hexadecyltrimethyl ammonium bromide modified gold nanoparticle dispersion to 10 types of heavy metal ions: understanding the involved molecules from experiment to simulation. *Langmuir* 29:7591–7599
9. Guo L, Xu Y, Ferhan AR, Chen G, Kim DH (2013) Oriented gold nanoparticle aggregation for colorimetric sensors with surprisingly high analytical figures of merit. *J Am Chem Soc* 135:12338–12345
10. Lu Y, Liu Y, Zhang S, Wang S, Zhang S, Zhang X (2013) Aptamer-based plasmonic sensor array for discrimination of proteins and cells with the naked eye. *Anal Chem* 85:6571–6574
11. Sang F, Li X, Zhang Z, Liu J, Chen G (2018) Recyclable colorimetric sensor of Cr³⁺ and Pb²⁺ ions simultaneously using a zwitterionic amino acid modified gold nanoparticles. *Spectrochim Acta A* 193:109–116
12. Yu Y, Hong Y, Wang Y, Sun X, Liu B (2017) Mercaptosuccinic acid modified gold nanoparticles as colorimetric sensor for fast detection and simultaneous identification of Cr³⁺. *Sensors Actuators B Chem* 239:865–873
13. Shahrivari S, Faridbod F, Ganjali MR (2018) Highly selective and sensitive colorimetric determination of Cr³⁺ ion by 4-amino-5-methyl-4H-1, 2, 4-triazole-3-thiol functionalized au nanoparticles. *Spectrochim Acta A* 191:189–194
14. Shellaiah M, Simon T, Venkatesan P, Sun KW, Ko FH, Wu SP (2018) Nanodiamonds conjugated to gold nanoparticles for colorimetric detection of clenbuterol and chromium (III) in urine. *Microchim Acta* 185:74
15. Guo JF, Huo DQ, Yang M, Hou CJ, Li JJ, Fa HB, Luo HB, Yang P (2016) Colorimetric detection of Cr (VI) based on the leaching of gold nanoparticles using a paper-based sensor. *Talanta* 161:819–825
16. Martinez AW, Phillips ST, Butte MJ, Whitesides GM (2007) Patterned paper as a platform for inexpensive, low-volume, portable bioassays. *Angew Chem Int Ed* 46:1318–1320
17. Pourreza N, Golmohammadi H, Rastegarzadeh S (2016) Highly selective and portable chemosensor for mercury determination in water samples using curcumin nanoparticles in a paper based analytical device. *RSC Adv* 6:69060–69066
18. Pourreza N, Golmohammadi H (2015) Application of curcumin nanoparticles in a lab-on-paper device as a simple and green pH probe. *Talanta* 131:136–141
19. Hosu O, Ravalli A, Piccolo GML, Cristea C, Sandulescu R, Marrazza G (2017) Smartphone-based immunosensor for CA125 detection. *Talanta* 166:234–240
20. Meredith NA, Quinn C, Cate DM, Reilly TH, Volckens J, Henry CS (2016) Paper based analytical devices for environmental analysis. *Analyst* 141:1874–1887
21. Devoy J, Géhin A, Müller S, Melczer M, Remy A, Antoine G, Sponne I (2016) Evaluation of chromium in red blood cells as an indicator of exposure to hexavalent chromium: an in vitro study. *Toxicol Lett* 255:63–70
22. Tsai TL, Kuo CC, Pan WH, Chung YT, Chen CY, Wu TN, Wang SL (2017) The decline in kidney function with chromium exposure is exacerbated with co-exposure to lead and cadmium. *Kidney Int* 92:710–720
23. Li Y, Wu P, Xu H, Zhang Z, Zhong X (2011) Highly selective and sensitive visualizable detection of Hg²⁺ based on anti-aggregation of gold nanoparticles. *Talanta* 84:508–512
24. Liu Y, Wang X (2013) Colorimetric speciation of Cr(III) and Cr(VI) with a gold nanoparticle probe. *Anal Methods* 5:1442–1448
25. Clesceri LS, Greenberg AE, Eaton AD (1998) Standard method for the examination of water and wastewater, 20th edn. United Book Press, Baltimore
26. Cerda V, Casassas E, Borrull F, Esteban M (1982) Thermometric behaviour of (methylthio) acetic, thiodiacetic and 3, 3'-thiodipropionic acids. *Thermochim Acta* 55:1–10
27. Langevin D, Raspud E, Mariot S, Knyazev A, Stocco A, Salonen A, Luch A, Haase A, Trouiller B, Rziel C, Lozano O (2018) Towards reproducible measurement of nanoparticle size using dynamic light scattering: important controls and considerations. *NanoImpact* 10:161–167
28. Chen W, Cao F, Zheng W, Tian Y, Xianyu Y, Xu P, Zhang W, Wang Z, Deng K, Jiang X (2015) Detection of the nanomolar level of total Cr [(III) and (VI)] by functionalized gold nanoparticles and a smartphone with the assistance of theoretical calculation models. *Nanoscale* 7:2042–2049
29. Jin W, Huang P, Chen Y, Wu F, Wan Y (2015) Colorimetric detection of Cr³⁺ using gold nanoparticles functionalized with 4-amino hippuric acid. *J Nanopart Res* 17:358
30. Wang X, Wei Y, Wang S, Chen L (2015) Red-to-blue colorimetric detection of chromium via Cr(III)-citrate chelating based on tween 20-stabilized gold nanoparticles. *Colloids Surf A Physicochem Eng Asp* 472:57–62
31. Li S, Wei T, Ren G, Chai F, Wu H, Qu F (2017) Gold nanoparticles based colorimetric probe for Cr(III) and Cr(VI) detection. *Colloids Surf A Physicochem Eng Asp* 535:215–224
32. Tahmasebi Z, Davarani SSH (2016) Selective and sensitive speciation analysis of Cr(VI) and Cr(III), at sub- $\mu\text{g L}^{-1}$ levels in water samples by electrothermal atomic absorption spectrometry after electromembrane extraction. *Talanta* 161:640–646
33. Elavarasi M, Rajeshwari A, Chandrasekaran N, Mukherjee A (2013) Simple colorimetric detection of Cr(III) in aqueous solutions by as synthesized citrate capped gold nanoparticles and development of a paper based assay. *Anal Methods* 5:6211–6218
34. Bhatt R, Bhatt R, Padmaja P (2018) DTPA capped gold and silver nanofluids-facile synthesis and their application as chromium sensors. *Sensor Actuat B-Chem* 258:602–611
35. Rahbar N, Salehnezhad Z, Hatamie A, Babapour A (2018) Graphitic carbon nitride nanosheets as a fluorescent probe for chromium speciation. *Microchim Acta* 185:101